J Therm Anal Calorim (2010) 101:907–911
DOI 10.1007/s10973-009-0551-0

Thermal behavior of the mixed composition xSb_2O_3–$(1 - x)Bi_2O_3$–$6(NH_4)_2HPO_4$

P. Melnikov · H. W. L. dos Santos · R. V. Gonçalves

Received: 28 August 2009 / Accepted: 7 October 2009 / Published online: 31 October 2009

Abstract The study of the system xSb_2O_3–$(1 - x)Bi_2O_3$–$6(NH_4)_2HPO_4$ has been carried out to identify the phases and simulate the mechanisms of their formation, using the technique of thermal analysis in association with X-ray diffractometry. The main stages observed during thermal treatment of the samples include: (1) elimination of water and ammonia leading to the formation of $(NH_4)_5P_3O_{10}$; (2) reaction of the latter with $M_2^{III}O_3$ and the formation of acidic polyphosphates $M_2^{III}H_2P_3O_{10}$; (3) their dehydration with the formation of the polyphosphates $M^{III}(PO_3)_3$. Then $Sb(PO_3)_3$ decomposes giving $SbPO_4$ and P_2O_5. In the presence of excessive P_2O_5, two moles of $Bi(PO_3)_3$ condensate into oxophosphates $Bi_2P_4O_{13}$ and BiP_5O_{14}. The data of thermal analysis match with the composition of intermediate and final products. The hygroscopicity of the samples diminishes with growing bismuth content.

Keywords Antimony phosphate · Bismuth phosphate · Thermal analysis

P. Melnikov (✉)
Department of Clinical Surgery, School of Medicine, UFMS, Caixa Postal 549, Campo Grande, MS, Brazil
e-mail: petrmelnikov@yahoo.com

H. W. L. dos Santos
Physics Institute, Federal University of Rio Grande do Sul, Porto Alegre, RS, Brazil

R. V. Gonçalves
Physics Department, CCET/UFMS, Caixa Postal 549, Campo Grande, MS, Brazil

Introduction

Antimony and bismuth orthophosphates, $SbPO_4$ and $BiPO_4$ are of utmost importance for the preparation of new materials due to the very specific structural arrangements of their crystalline compounds. Monoclinic $SbPO_4$ is built of the antimony polyhedra, which instead of oxygen atoms have lone electronic pairs at some of their apices. Therefore, Sb(III) coordination becomes 2 + 2 + E, where E is electronic pair. As a result, the Sb–Sb distances are so short that one can expect various phase transformations (e.g., *P21/m* → *P21*), as well as anomalous electrical and optical properties. These may be due to the stereochemical activity of either the electronic pairs or the polynuclear Sb_2 groups [1, 2]. Besides the conventional crystalline compound, a vitreous form of $SbPO_4$ has been obtained and its thermochemistry studied [3]. On the other hand, $BiPO_4$ was reported to have three polymorphs: a metastable trigonal form and two monazite-like modifications [4] with the structures different from $SbPO_4$. Monazite atomic arrangement [5] is based on {001} chains of intertwining phosphate tetrahedra and BiO_9 polyhedra. Vitreous form of $BiPO_4$ is unknown.

Under appropriate experimental conditions, crystalline $SbPO_4$, a compound without cation-exchange properties, has been claimed to give intercalation complexes with hydrazine, ethylenediamine and some other amines [6]. Later, a new layered oxo-antimony catecholate was obtained by treating $SbPO_4$ with aqueous catechol. This reaction seems to be reversible and catechol can be at least partly substituted for pyridine [7]. Despite the structural dissimilarities, $BiPO_4$ is also capable of intercalation of small molecules. At least one of the polymorph modifications is stabilized by $0.67H_2O$. This water is so important that its loss immediately provokes phase transition [4]. The

presence of active sites in both orthophosphates allowed their applications as good catalysts, [8, 9], ion-sensors [10], as well as for the coprecipitation and separation of radionuclides [11]. $BiPO_4$ is also known as a dopant of phosphate glasses largely improving their properties, such as ionic, electronic, and fast ionic conductivity [12]. However, to the best of our knowledge, there is no reports on the systems containing both antimony and bismuth phosphates, which may be the case in technological practice, e.g., for the fabrication of glasses with piezoelectric coefficients different from zero. Although the existence of solid solutions is difficult to expect, bismuth can "dilute" antimony compounds, lowering their hygroscopicity and thus rendering inorganic materials stable in air.

As the main method to obtain an active disordered $SbPO_4$ is through the decomposition of $Sb(PO_3)_3$ [13], it was decided to verify the possibility of coexistence of $SbPO_4$ and $BiPO_4$ by simulating the process of interactions in the system $x Sb_2O_3$–$(1 - x)Bi_2O_3$–$6(NH_4)_2HPO_4$ for the mixed compositions corresponding to the formation of both polyphosphates.

The aim of this study is to study the phases present during the thermal treatment of the samples $x Sb_2O_3$–$(1 - x)Bi_2O_3$–$6(NH_4)_2HPO_4$ and mechanisms of their formation using the technique of thermal analysis in association with X-ray diffraction.

Experimental

Starting reagents were ammonium hydrogen phosphate $(NH_4)_2HPO_4$, antimony(III) oxide, and Bi(III) oxide, all of analytical grade purity purchased from Merck. Thermal behavior was studied by thermal gravimetric analysis (TGA) and differential scanning calorimetry (DSC), both 50H Shimadzu Instrumentation. Preparations were simulated by mixing up starting materials and heating the test specimens (4–6 mg) up to 900 °C in the flux of synthetic air at the rate 10 °C min^{-1}. Mass losses during heating were analyzed and compared to previously calculated values. X-ray diffraction patterns were registered with a Siemens Kristalloflex diffractometer with a graphite diffracted beam monochromator and Ni filter. All compounds separately prepared in static conditions were identified by comparison of experimental X-ray patterns with available ISDD database files.

Batch compositions were prepared using increasing amounts of bismuth oxide, with intervals of 10% by mol. The quantities were calculated according to the compositions $x Sb_2O_3 + (1 - x)Bi_2O_3 + 6(NH_4)_2HPO_4$, where $x = 0.9$–0.1. After grinding in an agate mortar, the powders were heated at 180 °C for 30 min, at 300 °C for 60 min, and then at 800 °C for 240 min. Such a prolonged heating at 800 °C is needed due to poor diffusion conditions at this temperature. The treatment was carried out in air at the rate 15 °C min^{-1}. In addition, masses of the samples were measured after exposing them to room moisture.

Results and discussion

Thermal analysis

The TG curves of the mixtures $x Sb_2O_3$–$(1 - x)Bi_2O_3$–$6(NH_4)_2HPO_4$ (Fig. 1) are similar until ~400 °C. Three net endothermic effects can be seen, corresponding to mass losses presented in Table 1 in accordance with the values calculated for the formation of intermediate compounds. These calculations were carried out invariably taking into account the presence of $Me_2^{III}O_3$ in the starting mixtures. As the only volatile products can be ammonia and water, it means that during the thermal treatment the ratio cations/anions is automatically diminished, and we deal with the process of $(NH_4)_2HPO_4$ polycondensation [14, 15].

In contrast to the condensation of $NH_4H_2PO_4$ [13], the usage of $(NH_4)_2HPO_4$ leads to the elimination of only 2 and 4 moles of NH_3 and 4 moles of H_2O. The calculated values for these mass losses fit the following reaction scheme:

$$6(NH_4)_2HPO_4 = 2(NH_4)_5P_3O_{10} + 2NH_3 + 4H_2O$$

Therefore, at this first step, only ammonium tripolyphosphate is formed and the remaining Sb_2O_3 and Bi_2O_3 are kept up intact.

At the second step, Sb_2O_3 and Bi_2O_3 react with ammonium tripolyphosphate. As a result, five ammonium ions are replaced by one trivalent metal ion and two protons. These mass losses suggest the following process:

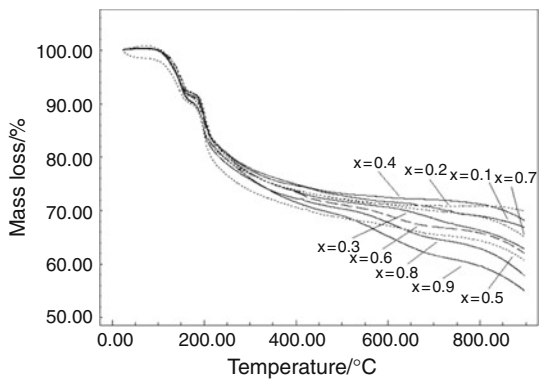

Fig. 1 TG curves simulating the processes in the system $x Sb_2O_3$–$(1 - x)Bi_2O_3$–$6(NH_4)_2HPO_4$

Table 1 Mass losses at different stages of thermal treatment calculated in relation to the initial sum of $6(NH_4)_2HPO_4$ and $M^{III}_2O_3$

x	Mass loss/%					
	$(NH_4)_5P_3O_{10}$		$M^{III}H_2P_3O_{10}$		$M^{III}(PO_3)_3$	
	Calc.	Exp.	Calc.	Exp.	Calc.	Exp.
0.1	8.5	8.7	18.1	20.0	25.2	26.6
0.2	8.7	8.6	18.3	18.3	25.5	25.5
0.3	8.8	9.2	18.6	19.9	25.9	28.0
0.4	8.9	8.7	18.9	20.2	26.3	26.6
0.5	9.1	9.0	19.1	20.3	26.7	28.3
0.6	9.2	9.3	19.4	19.2	27.1	27.8
0.7	9.3	9.1	19.7	20.6	27.5	27.4
0.8	9.5	10.0	20.0	21.0	27.9	28.6
0.9	9.6	10.0	20.4	20.59	28.3	29.7

$$2(NH_4)_5P_3O_{10} + M^{III}_2O_3 = 2M^{III}H_2P_3O_{10} + 10NH_3 + 3H_2O$$

As can be easily seen, acidic polyphosphates monohydrates $M^{III}H_2P_3O_{10}$ and polyphosphate monohydrates $M^{III}(PO_3)_3{\cdot}H_2O$ have identical composition and therefore can be regarded as a rare case of inorganic isomers. Similar results were recently obtained in the case of rare earth polyphosphates [16] showing that the cationic radii are of no importance in this line of transformations.

At the third step, $M^{III}(PO_3)_3{\cdot}H_2O$ lose water and are converted into polyphosphates:

$$2M^{III}H_2P_3O_{10} = 2M^{III}(PO_3)_3 + 2H_2O$$

Differential scanning calorimetry (DSC) curves of the same mixtures are represented in Fig. 2. The superposed TG and DSC curves for the sample with $x = 6$ are given in Fig. 3.

Both graphics confirm the above scheme of chemical interactions showing two net endothermic effects at 160 and 201 °C, which correspond to the dehydration and ammonia elimination processes.

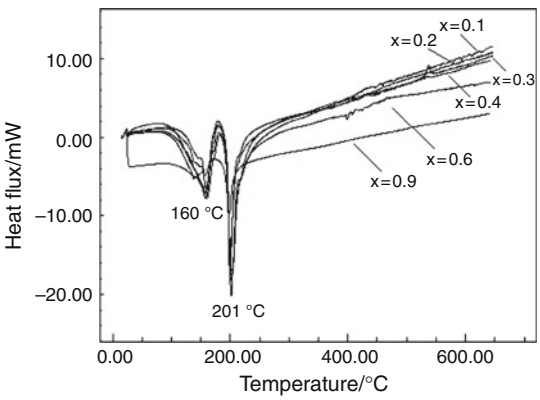

Fig. 2 Comparison of DSC curves for different x

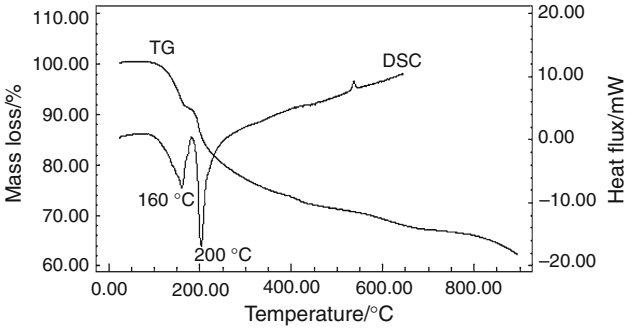

Fig. 3 Superposition of TG and DSC curves for the sample with $x = 0.6$

The last mass loss is revealed only as change of slope. It is possible that thermal effects of isomer transformation, dehydration, and polyphosphates crystallization are mutually compensated in a narrow temperature range. At this stage, X-ray technique is of no help because the polyphosphates formed have vitreous arrangement giving patterns of amorphous products.

As can be seen in Fig. 1, at higher temperatures, the process of mass loss continues, but the similarities in the shape of curves are not so evident. According to the behavior of pure vitreous $Sb(PO_3)_3$ [13], this late mass loss should be due to the vaporization of P_2O_5 with the parallel formation of $M^{III}PO_4$. However, these thermogravimentric data do not fit the suggested hypothesis: the real mass losses never reach the values calculated for the total conversion of polyphosphates into orthophosphates. This clearly indicates that somehow phosphorus pentoxide is being retained when bismuth is present. Moreover, no noticeable exothermic effects are observed, meaning that kinetics is determined by the shift of equilibrium in decomposition process and should depend on the vapor pressure of P_2O_5 at a given temperature.

X-ray diffractometry

The results of phase analysis are given in Table 2. X-ray powder diffraction of the samples obtained during static heating at 800 °C allowed making understandable the mechanisms involved. Figure 4 shows a family of diffractograms corresponding to $x = 0.9 - 0.1$. It can be seen that they all share at least one crystalline phase. The sample with $x = 0.2$ is an exception because the material is practically amorphous. Phase analysis carried out using ICDD database showed (Table 2) that we deal with monoclinic $SbPO_4$ with lattice parameters $a = 5.106$ Å, $b = 6.772$ Å, $c = 4.745$ Å, and $\beta = 94.61°$ (ICDD file 35-0829). The experimental parameters calculated on the basis of diffractograms remained unchanged within standard deviation, meaning that no solid solutions exist in this range of x.

The apparent inconsistency in intensities and/or order–disorder geometry may be explained assuming that after 400 °C the crystallization processes strongly depend on diffusion in porous mass, which is formed after gaseous NH_3 and H_2O vaporization. The number and distribution of these pores is difficult to control, therefore these processes may be long, incomplete and do not guarantee sufficient homogeneity.

As to the crystalline bismuth compounds, with the exception of $x = 0.1$, they are represented by two minority phases, which are bismuth oxophosphates $Bi_2P_4O_{13}$ and BiP_5O_{14}. Their X-ray patterns were identified by comparison with ICDD files 30-0192 and 36-0006.

In this case, polymeric bismuth oxophosphates with the ratios Bi/P = 1:2 and 1:5 are formed from $Bi(PO_3)_3$ which holds Bi/P = 1:3, therefore the whole reaction can be written as:

$$3Bi(PO_3)_3 = Bi_2P_4O_{13} + BiP_5O_{14}$$

This explains the absence of $BiPO_4$ reflections and at the same time the incompleteness of P_2O_5 removal seen on TG curves.

Only for the sample poorest in antimony ($x = 0.1$), that is in the absence of excessive P_2O_5, crystalline $BiPO_4$ is available as the majority phase (ICDD file 43-0637). In this case, antimony is present as traces in the forms of $SbPO_4$ and $Sb_2(P_2O_7)_2$ (ICDD 84-1675). The latter compound (mixed-valence pyrophosphate) is the only oxidized form found. No reflections could have been attributed to bismuth antimonate, $BiSbO_4$.

Evaluation of hygroscopicity

As described elsewhere [14, 15], antimony polyphosphate and vitreous antimony polyphosphate are extremely hygroscopic compounds making difficult their applications. Using the partially substituted samples, we proceeded with the study of their behavior in respect to the moisture content of the air, controlling mass gain (Fig. 5).

Table 2 Phase analysis of the mixed compositions xSb_2O_3–$(1 - x)$ Bi_2O_3–$6(NH_4)_2HPO_4$

x	Majority crystalline phases	Minority crystalline phases
0.9	$SbPO_4$	–
0.8	$SbPO_4$	BiP_5O_{14} and $Bi_2P_4O_{13}$
0.7	$SbPO_4$	BiP_5O_{14} and $Bi_2P_4O_{13}$
0.6	$SbPO_4$	BiP_5O_{14} and $Bi_2P_4O_{13}$
0.5	$SbPO_4$	BiP_5O_{14} and $Bi_2P_4O_{13}$
0.4	$SbPO_4$	BiP_5O_{14} and $Bi_2P_4O_{13}$
0.3	$SbPO_4$	BiP_5O_{14} and $Bi_2P_4O_{13}$
0.2	Amorphous sample	
0.1	$BiPO_4$	$SbPO_4$ and $Sb_2(P_2O_7)_2$

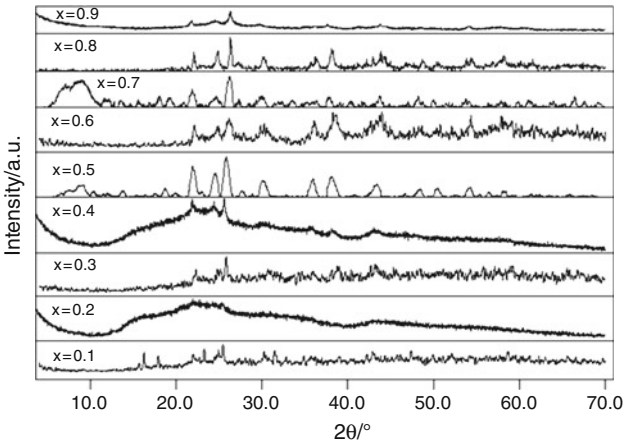

Fig. 4 X-ray powder diffractograms of the samples with different x after heating at 800 °C

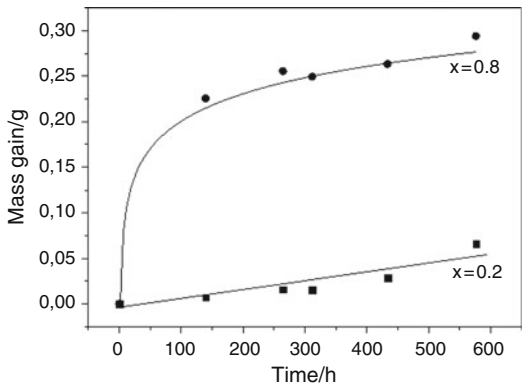

Fig. 5 Comparison of mass gain versus time by the mixtures with $x = 0.2$ and 0.8

Two representative samples were chosen corresponding to the major and minor bismuth content in the batch ($x = 0.2$ and 0.8). The samples were exposed to the laboratory air during 600 h. At the end of the exposure, mass gain for the composition with $x = 0.8$ (poor in bismuth) reached 22.0%, while for $x = 0.2$ (rich in bismuth) it was only 10.7%, neither instant hydrolysis was observed. It means that in the long run bismuth permits to protect the samples from moisture. These data represent only preliminary evaluation and investigations are in progress.

Conclusions

The processes occurring in the system xSb_2O_3–$(1 - x)$ Bi_2O_3–$6(NH_4)_2HPO_4$ include the formation of intermediate polyphosphate $(NH_4)_5P_3O_{10}$ and tripolyphosphate M^{III+} $SbH_2P_3O_{10}$. Then individual polyphosphates $Sb(PO_3)_3$ and

$Bi(PO_3)_3$ are formed. Due to the redistribution of excessive P_2O_5, two moles of $Bi(PO_3)_3$ condensate into oxophosphates $Bi_2P_4O_{13}$ and BiP_5O_{14}. X-ray diffraction of crystalline samples obtained in static conditions confirms phase compositions supposed on the basis of TG and DSC curves. The hygroscopicity of the samples diminishes with growing bismuth content.

References

1. Kinberger B. Crystal structure of antimony phosphate. Acta Chem Scand. 1970;214:320–8.
2. Kurbanov KM. On crystal structure of antimony phosphate $SbPO_4$. Kristallografia. 1987;32:1265–7.
3. Melnikov P, Secco MAC, Guimarães WR, dos Santos HWL. Thermochemistry of vitreous antimony orthophosphate. J Therm Anal Calorim. 2008;92:579–82.
4. Romero B, Bruque S, Aranda MAG, Iglesias JE. Syntheses, crystal structures, and characterization of bismuth phosphates. Inorg Chem. 1994;33:1869–74.
5. Ni Yu, Hughes JM, Mariano AN. Crystal-chemistry of the monazite and xenotime structures. Am Mineral. 1995;80:21–6.
6. Saadouri H, Boukhari A, Flandrois S, Aristide J. Intercalation of hydrazine and amines in antimony phosphate. Mol Cryst Liq Cryst. 1994;244:173–6.
7. Alonzo G, Bertazzi N, Galli P, Marci G, Massucci MA, Palmisano L, et al. In search of layered antimony(III) materials: synthesis and characterization of oxo-antimony(III) catecholate and further studies on antimony(III) phosphate. Mater Res Bull. 1998;33:1233–40.
8. Chang TS, Li GJ, Shin CH, Lee YK, Yun SS. Catalytic behavior of $BiPO_4$ in the multicomponent bismuth phosphate system on the propylene ammoxidation. Catal Lett. 2000;68:229–34.
9. Takita Y, Ninomiya M, Miyake H, Wakamatsu H, Yoshinaga Y. Catalytic decomposition of perfluorocarbons: Part II—decomposition of CF_4 over $AlPO_4$-rare earth phosphate catalysts. Phys Chem Chem Phys. 1999;1:4501–4.
10. Iitaka K, Tani Y, Umezawa Y. Orthophosphate ion-sensors based on a quartz-crystal microbalance coated with insoluble orthophosphate salts. Anal Chim Acta. 1997;338:77–87.
11. Charyulu MM, Chetty KV, Phal DG, Sagar V, Naronha DM, Pawar SM, et al. Recovery of americium from nitric acid solutions containing calcium by different co-precipitation methods. J Rad Nucl Chem. 2002;251:153–4.
12. Jermoumi T, Hafid M, Et-tabirou M, Taibi M, ElQadim H, Toreis N. Electrical conductivity study on Na_3PO_4–$Pb_3(PO_4)_2$–$BiPO_4$. Mater Sci Eng B. 2001;85:28–33.
13. Melnikov P, dos Santos FJ, Santagnelli SB, Secco MAC, Guimarães WR, Delben A, et al. Mechanism of the formation and properties of antimony polyphosphate. J Therm Anal Calorim. 2005;81:45–9.
14. Kulaev IS, Vagabov VM, Kulakovskaya TV. The structure of condensed phosphates. In: Kulaev IS, Vagabov VM, Kulakovskaya TV, editors. The biochemistry of inorganic polyphosphates. New York: Wiley; 2004.
15. Van Wezer JR. Phosphorus and its compounds, vol. 1. New York: Interscience Publishers; 1958.
16. Melnikov P, Guirardi AL, Secco MAC, de Aguiar EN. Study of trivalent elements polyphosphates by thermal analysis. J Therm Anal Calorim. 2008;94:162–7.